UNIVERSIDADE FEDERAL DE MINAS GERAIS
Escola de Engenharia
Colegiado do Curso de Graduação em Engenharia ...

Nome da pessoa autora

TÍTULO DO TRABALHO

Belo Horizonte
2024

Nome da pessoa autora

TÍTULO DO TRABALHO

Trabalho de Conclusão de Curso apresentado ao Curso de Engenharia de Sistemas da Universidade Federal Minas Gerais, como requisito parcial para o grau de bacharel (a) em Engenharia de Sistemas.

Orientadora: Profa. Dra. Fulana Beltrano

Coorientador: Prof. Dr. Ciclano da Silva

Belo Horizonte
2024

Troque pelo arquivo PDF da ficha catalográfica após obtê-la da biblioteca da sua unidade.

Troque pelo arquivo PDF da folha de aprovação ou ata de defesa após obtê-la do seu programa de pós-graduação (após a defesa).

Esse trabalho é dedicado à aquela pessoa.

Agradecimentos

Você pode escrever aqui os agradecimentos a pessoas que contribuíram para a realização do trabalho.

“Aqui vai uma bela e inspiradora frase.”

Resumo

Escreva aqui o resumo do seu trabalho.

Palavras-chave: palavra-chave 1; palavra-chave 2; palavra-chave 3.

Abstract

Translate here the abstract of your work.

Keywords: keyword 1; keyword 2; keyword 3.

Lista de Siglas e Símbolos

Siglas

ACO	Ant Colony Optimization
BIM	Born Iterative Method
CNN	Convolutional Neural Networks
DE	Differential Evolution
EA	Evolutionary Algorithm
GA	Genetic Algorithm
GAN	Generative Adversarial Network
PSO	Particle Swarm Optimization
TMz	Modo Magnético Transversal em z

Símbolos

ε	Permissividade complexa [F/m + $j\Omega$/m]
ε_r	Permissividade relativa
θ	Ângulo da coordenada polar [rad]
λ_b	Comprimento de onda de fundo [m]
σ	Condutividade [Ω/m]
ϕ	Ângulo de incidência [rad]
$\mathbf{E}$	Vetor de intensidade elétrica [V/m]
E_z	Componente z do vetor de intensidade elétrica [V/m]
k	Número de onda [1/m]
$\mathbb{R}$	Conjunto dos números reais
$\mathbf{r}$	Vetor posição no espaço 3D [m]
x, y, z	Coordenadas cartesianas [m]
V	Espaço tridimensional

Sumário

Capítulo 1

Introdução

Parte inicial do texto na qual se apresenta a delimitação do assunto tratado, os objetivos da pesquisa e outros elementos necessários para apresentar o tema do trabalho. O texto tem o objetivo de introduzir o leitor ao trabalho e apresentar as informações para uma compreensão geral da proposta desenvolvida.

1.1 Objetivos Geral e Especíificos

Descrever os objetivos geral e específicos do trabalho. O objetivo geral devem ser claro e conciso, indicando o propósito do trabalho. Os objetivos específicos devem ser apresentados de forma a indicar os passos necessários para atingir o objetivo geral. Geralmente, em formato de tópicos.

1.2 Contribuições e Originalidade

Descrever as contribuições do trabalho, indicando o que o trabalho propõe de novo ou diferente em relação ao estado da arte. As contribuições devem ser claras e objetivas, indicando o que o trabalho agrega ao conhecimento existente.

1.3 Organização do Trabalho

Descrever a organização do trabalho, indicando o conteúdo de cada capítulo e a relação entre eles. A organização do trabalho deve ser clara e coerente, de forma a facilitar a compreensão do leitor.

Capítulo 2

Revisão Bibliográfica

Ao redigir uma revisão bibliográfica em trabalhos acadêmicos, é crucial adotar uma abordagem sistemática e crítica. Inicie identificando e selecionando fontes relevantes que abordem diretamente o tema de pesquisa, priorizando publicações acadêmicas revisadas por pares, como artigos de periódicos, livros e conferências. Uma boa prática é organizar a literatura em temas ou escolas de pensamento, facilitando a compreensão do leitor sobre o estado da arte e as lacunas existentes. É importante também avaliar criticamente cada obra, discutindo sua contribuição para o campo, metodologias, resultados e limitações. A revisão deve ser escrita de forma coesa, com transições suaves entre os trabalhos discutidos, e deve terminar destacando como a pesquisa atual se insere e contribui para o conhecimento existente. Citando adequadamente todas as fontes, evita-se o plágio e reconhece-se o trabalho dos pesquisadores originais, além de fornecer ao leitor caminhos para aprofundamento.

Capítulo 3

Metodologia

Redigir um capítulo sobre metodologia em um trabalho acadêmico é fundamental para demonstrar a validade e a confiabilidade da pesquisa. Este capítulo deve detalhar os procedimentos e técnicas utilizados para coletar e analisar dados, permitindo que outros pesquisadores reproduzam o estudo. Aqui estão os passos essenciais para escrever um capítulo de metodologia eficaz:

- Introdução à Metodologia: Comece com uma breve introdução que esclareça o propósito do capítulo e como ele contribui para os objetivos gerais da pesquisa.
- Descrição da Pesquisa: Especifique o tipo de pesquisa realizada (qualitativa, quantitativa, mista) e justifique a escolha. Explique como essa abordagem é adequada para responder às perguntas de pesquisa ou hipóteses.
- Participantes ou Dados: Descreva a população-alvo, critérios de inclusão e exclusão, e como os participantes ou dados foram selecionados. Para pesquisas experimentais, explique como os grupos de controle e experimentais foram formados.
- Instrumentos e Materiais: Liste os instrumentos, ferramentas, ou materiais utilizados na coleta de dados, incluindo questionários, entrevistas, software, etc. Descreva como e por que cada instrumento foi escolhido.
- Procedimento: Detalhe todos os passos seguidos durante a coleta de dados. Para experimentos, descreva as condições sob as quais foram realizados, incluindo variáveis controladas e não controladas.
- Análise de Dados: Explique as técnicas estatísticas, métodos de análise qualitativa, ou modelos utilizados para analisar os dados coletados. Justifique a escolha desses métodos e discuta sua adequação para o tipo de dados coletados.
- Validade e Confiabilidade: Discuta as medidas tomadas para garantir a validade e confiabilidade dos resultados. Isso pode incluir a validação de instrumentos, triangulação de dados, ou testes piloto.
- Limitações: Reconheça quaisquer limitações metodológicas que possam afetar os resultados ou a interpretação da pesquisa.
- Ética: Se aplicável, descreva as considerações éticas relacionadas à pesquisa, incluindo

aprovações de comitês de ética, consentimento informado dos participantes, e como a privacidade e a confidencialidade foram mantidas.

- Resumo: Conclua o capítulo com um resumo dos pontos-chave, reforçando como a metodologia adotada permite abordar as perguntas de pesquisa ou testar as hipóteses.

Lembre-se de que a clareza e a precisão são cruciais neste capítulo. O objetivo é fornecer informações suficientes para que outros pesquisadores possam entender como o estudo foi conduzido e, se desejado, replicar a pesquisa.

Capítulo 4

Resultados

Escrever um capítulo de resultados em trabalhos acadêmicos é uma etapa crucial, pois comunica as descobertas da pesquisa. Aqui estão algumas sugestões para estruturar e redigir este capítulo de forma eficaz:

- Introdução Breve: Comece com uma introdução curta que reitere os objetivos da pesquisa e explique o que será apresentado no capítulo.
- Organização Lógica: Estruture o capítulo de forma lógica, geralmente seguindo a ordem das perguntas de pesquisa ou hipóteses. Isso ajuda os leitores a acompanhar facilmente as descobertas.
- Apresentação Clara dos Dados: Apresente os resultados de maneira clara e concisa. Use tabelas, gráficos e figuras para ilustrar os dados de forma eficaz, garantindo que cada um seja claramente rotulado e acompanhado de uma legenda explicativa.
- Descrição dos Resultados: Forneça uma descrição textual dos resultados, destacando as descobertas principais.
- Referência aos Objetivos e Hipóteses: Faça referência explícita aos objetivos da pesquisa ou hipóteses ao apresentar os resultados, indicando como cada resultado se relaciona com eles.
- Precisão e Objetividade: Mantenha a precisão e objetividade ao relatar os resultados. Evite usar linguagem emotiva ou fazer inferências sem suporte dos dados.
- Tratamento de Dados Negativos ou Inesperados: Se houver resultados negativos ou inesperados, inclua-os e ofereça uma breve descrição. Esses resultados podem ser tão informativos quanto os positivos.
- Uso de Subseções: Divida o capítulo em subseções, se necessário, para manter a organização e facilitar a leitura. Cada subseção pode abordar diferentes aspectos dos resultados.
- Consistência com Metodologia: Garanta que a apresentação dos resultados seja consistente com a metodologia descrita anteriormente. Isso inclui o uso dos mesmos termos e definições.
- Sumário dos Resultados: Conclua o capítulo com um sumário dos principais resultados.

Capítulo 5

Conclusion

This chapter concludes the thesis. Firstly, a recapitulation of the main topics explored in the thesis is presented in Section 5.1. This serves as a concise summary, highlighting the main ideas, proposals, key findings, and their significance within the research context. By revisiting the main research questions and objectives, the recapitulation provides a holistic view of the thesis's scope and accomplishments.

Following the recapitulation, a critical analysis of the research methodology, limitations, and potential biases is presented in Section 5.2. Self-criticism plays a crucial role in research as it allows for a reflective assessment of the strengths and weaknesses of the study. By acknowledging any limitations or areas for improvement, this section contributes to the overall integrity and maturity of the research project.

Next, the chapter discusses the proposal continuity in Section 5.3. In the continuity proposals, different ideas are described that can be addressed after this project. The topics are developments of subjects that were part of the work, which could receive more attention and could contribute to the literature. Lastly, the chapter concludes with a list of the bibliographic production generated during the project (Section 5.4).

5.1 Recapitulation

Microwave imaging is a significant inverse problem with applications in various fields such as defect identification in structures, through-wall imaging, cancer detection, among others. It involves reconstructing the interior of inaccessible regions based on field measurements at microwave frequencies and images derived from the electrical properties of the materials within the investigated space.

This thesis aimed to comprehensively review the mathematical aspects of the problem, recognizing that microwave imaging is an electromagnetic inverse scattering problem. The objective is to determine the cause, i.e., one or more scatterers, of the observed effect, i.e., the scattered field. Maxwell's Equations provide integral equations that relate the observed scattered field outside the region of interest with the unknown electromagnetic field and the mapping of electrical properties inside the region. However, this relationship is nonlinear due to the unknown nature of the electromagnetic field and the mapping of electrical properties, requiring simultaneous resolution of both variables.

The inverse problem is known to be ill-posed, lacking a unique solution or continuity in the relationship between the scattered field and the imaged medium. To address this, various formulas, including traditional integral formulas, have been developed to mitigate the inherent challenges of the problem. The degree of nonlinearity increases with the number of scatterers or their contrast, further complicating the solution process.

The thesis also presented an extensive overview of numerical methodologies to solve the problem, covering topics such as discretization, linear approximations, and regularization methods for ill-posed systems of equations. In the literature, numerical methods for the inverse electromagnetic scattering problem are classified into qualitative and quantitative methods. Qualitative methods focus on reconstructing the shape of scatterers, while quantitative methods aim to estimate the electrical properties in addition to recovering their geometries.

Noteworthy within qualitative methods is the Orthogonality Sampling Method (OSM), capable of recovering scatterer geometry and detecting different contrast levels. On the other hand, quantitative methods can be further categorized as deterministic or stochastic, depending on whether they rely on well-defined sequences of steps or stochastic processes. Deep Learning techniques have gained attention for their potential in enabling real-time imaging. Additionally, the application of Surrogate Models to assist algorithms for the problem, particularly those dependent on forward problem simulations, is an emerging area that holds promise in reducing computational costs while requiring effective representation methods.

The thesis also identified others shortcomings in the field, such as the lack of an integrated platform for algorithm development and testing, the need for standardized performance indicators, and limited generalization capacity in experimental designs. To address these issues, the thesis proposed two main propositions in the two-dimensional case of the electromagnetic inverse problem.

The first proposal involved applying Surrogate Models to assist Evolutionary Algorithms and Descent Methods, utilizing images generated by the OSM qualitative method for representing solutions. Such approach implies in transforming the inverse problem into a two-dimensional optimization problem, allowing for efficient treatment by Surrogate Models and achieving greater precision than similar proposals in the literature (Salucci et al., 2022). Five formulations for surrogate model-assisted algorithms were proposed, utilizing both evolutionary and descent algorithms.

The second proposal focused on implementing a comprehensive algorithm development and testing structure that supports experimental design, quantification, and performance comparison of algorithms for the problem. This structure included software with object-oriented features capable of conducting case studies and benchmarking, a less explored area in the literature. The software facilitated exploring different problem characteristics, measuring various aspects of obtained images, and performing statistical comparisons to evaluate results more robustly.

The computational experiments conducted in the thesis included both case studies and benchmarking. The case studies covered four problem scenarios: simple, multiple, nonhomogeneous, and strong scatterers. In these studies, the proposed methods were compared against traditional deterministic methods. The benchmarking study focused on evaluating the performance of the proposed algorithms, specifically considering increasing object contrast levels.

The computational experiments conducted in this thesis provided valuable insights into the performance of algorithms assisted by surrogate models for microwave imaging. In general, the results indicated that these proposed algorithms have the capability to obtain images with comparable or slightly better qualities than traditional methods in the simplest cases. However, this improvement comes at a slightly higher computational cost in some instances.

One of the notable findings was that in high-contrast scenarios, the methodology assisted by surrogate models was able to reconstruct objects that traditional methods struggled with, all while maintaining a reasonable computational cost. This suggests that the surrogate models have the potential to address the limitations of traditional techniques and enable the imaging of challenging objects. It was also observed that the limitations of OSM posed restrictions on the application of the proposed methodology, particularly when dealing with numerous scatterers and varying levels of contrast. This highlights the need to consider the limitations of the qualitative method when applying the proposed approach.

In terms of the performance comparison between different algorithm versions, one of the evolutionary versions (SAEA2) demonstrated better image quality indicators but at a higher computational cost. On the other hand, a version based on the descent method (SADM2) showed comparable results in terms of image quality indicators while requiring significantly fewer computational resources. This finding suggests that a descent-based approach may offer a good balance between performance and computational efficiency.

Based on these results, it is evident that the application of surrogate models in the transformation of the inverse problem into a two-dimensional optimization problem is highly feasible. The objective function becomes much easier to predict using surrogate models, enabling the solution of scenarios where traditional techniques struggle to reconstruct images. The advantage of the approach lies in the reduced number of variables, which can be effectively handled by surrogate models. However, it is important to acknowledge that the limitations of OSM in certain scenarios prevent a more general application of the proposed methodology, unlike what is achievable with existing techniques in the literature (Salucci et al., 2022).

These promising results encourage further development of the technique of applying surrogate models to strike a better balance between the number of variables that the surrogate model must handle and the ability to generalize to more complex scattering scenarios. By refining the application of surrogate models, it may be possible to overcome current limitations and expand the scope of microwave imaging, opening new avenues for improved imaging performance in challenging environments.

5.2 Self-Criticism

Some critical points in conducting this research are commented below:

- In this work, a case study based on real measurements from the Fresnel Institute (Geffrin et al., 2005), which is commonly used in the literature, was not considered. Although including this case study could provide additional support for the real-world applicability of the proposed methodology, it was not feasible due to the slight differences in the electromagnetic propagation model used in the data. Adapting the model would require substantial time and effort, which was not available during the completion of this work.
- Regarding the benchmark study, the option was made to be more succinct and focus on the proposed methods. Therefore, the traditional deterministic methods were not included in the analysis. While including these methods would have allowed for a more comprehensive comparison, it would have increased the number of graphs and data to analyze, which was not the primary objective of this study.
- Salucci et al. (2022) presented the only methodology available in the literature that applied surrogate models to the problem, and this work frequently cites their contribution to contextualize its own. However, the methodology proposed by them was not implemented in this study. It would have been interesting to include their methodology in the comparison to evaluate the efficiency of the transformation into a two-dimensional optimization problem and identify scenarios where their approach may outperform the one proposed in this work.
- In the obtained results, it was observed that the formulations based on the SAEAs took longer to run, even when the number of evaluations had the same limit than SADMs. This suggests that the evolutionary operations employed in the algorithm may have a significant impact on the overall computational cost. Further investigation would be necessary to implement optimizations and improve the performance of these algorithms in terms of computational efficiency.

5.3 Continuity Proposals

There are some topics that can be further explored in a future work:

- **Improvements to the initial image approach**: In this work, one of the evident needs is to expand the scope of application of OSM to address more challenging scenarios effectively. This requires modifying equations (**??**)-(**??**) to enhance the method's robustness against highly nonlinear problems. One approach could be exploring new integral equations (Bevacqua and Isernia, 2021) or investigating efficient domain decomposition techniques (Zhang et al., 2022). Another alternative could be developing more efficient ways to obtain an initial image while controlling the computational cost.

- **A better elaborated comparative study addressing traditional deterministic methods**: The implementation of a benchmark tool opens up possibilities for a more elaborate experimental design to quantitatively describe the average performance of traditional deterministic methods using the proposed indicators. This type of study is currently lacking in the literature and could provide valuable insights into the differences between these algorithms when subjected to a comprehensive comparison.
- **Creation of standard test sets**: Creating a standard test suite would be beneficial to the field, as it would enable researchers to compare their algorithms using well-defined and meaningful scenarios. This standardized approach would facilitate future studies by multiple authors, ensuring consistency and facilitating comparisons.
- **Creation of test sets based on DNL value**: Furthermore, it would be advantageous to design a problem generation mechanism based on a DNL target value. This mechanism would enable studies analyzing the variation of performance indicators of algorithms with varying DNL. Machine learning techniques could be employed to predict the DNL using only the characteristics of the desired problem, further enhancing the efficiency of these investigations.
- **Limits of application of the methods**: During the experiments in this work, it was observed that DNL alone is not always sufficient to quantify the difficulty of solving a particular problem for an algorithm. In some cases, algorithms may struggle to solve problems with lower DNL while being able to solve higher DNL problems. It would be valuable to develop a way to quantify the application limits of an algorithm, taking into account the problem's specific characteristics. This approach would provide a more comprehensive description of the operating limits of each method.
- **Implementation of the 3D model**: To continue this work, formulating a standard definition for the three-dimensional problem and implementing a library capable of supporting and adapting the development and testing of algorithms in this context would be valuable. Additionally, implementing the methodology proposed in this work in its three-dimensional version would further extend its applicability and provide insights into its performance in more complex scenarios.

5.4 Bibliographic Production

Journals:

- Batista, A. C., Batista, L. S., & Adriano, R. (2021). A quadratic programming approach for microwave imaging. *IEEE Transactions on Antennas and Propagation, 69(8)*, 4923-

4934.

- Vargas, J. O., Batista, A. C., Batista, L. S., & Adriano, R. (2021). On the computational complexity of the conjugate-gradient method for solving inverse scattering problems. *Journal of Electromagnetic Waves and Applications, 35(17)*, 2323-2334.
- Batista, A. C., Adriano, R., & Batista, L. S. (2021). EISPY2D: An Open-Source Python Library for the Development and Comparison of Algorithms in Two-Dimensional Electromagnetic Inverse Scattering Problems. *arXiv preprint arXiv:2111.02185*. **Under review**.

Conferences:

- Vargas, J. O., Batista, A. C. ; Batista, L. S., Adriano, R. A Fast Conjugate Gradient Method for Solving Two-Dimensional Electromagnetic Inverse Scattering Problems. *XX Simpósio Brasileiro de Micro-Ondas e Optoeletrônica, 2022, Natal, RN*. Anais do XX Simpósio Brasileiro de Micro-Ondas e Optoeletrônica, 2022.

Referências Bibliográficas

Bartle, R. G. (1995). *The elements of integration and Lebesgue measure*, volume 27. John Wiley & Sons, Ltd.

Bevacqua, M. T. and Isernia, T. (2021). Quantitative non-linear inverse scattering: A wealth of possibilities through smart rewritings of the basic equations. *IEEE Open Journal of Antennas and Propagation*, 2:335–348.

Chew, W. (2009). *Integral equation methods for electromagnetic and elastic waves*. Morgan & Claypool Publishers, San Rafael, Calif.

Chew, W. C. (1995). *Waves and Fields in Inhomogeneous Media*. IEEE Press.

Deb, K., Pratap, A., Agarwal, S., and Meyarivan, T. (2002). A fast and elitist multiobjective genetic algorithm: Nsga-ii. *IEEE transactions on evolutionary computation*, 6(2):182–197.

Geffrin, J.-M., Sabouroux, P., and Eyraud, C. (2005). Free space experimental scattering database continuation: experimental set-up and measurement precision. *Inverse Problems*, 21(6):S117–S130.

Kellogg, O. D. (1953). *Foundations of potential theory*, volume 31. Courier Corporation.

Kirsch, A. (2011). *An Introduction to the Mathematical Theory of Inverse Problems*. Number 120 in Applied Mathematical Science. Springer, Verlag, NY, 2 edition.

Lebedev, L. P., Vorovich, I. I., and Gladwell, G. (1996). *Functional Analysis - Applications in Mechanics and Inverse Problems*. Number 41 in Solid Mechanics and Its Applications. Springer, Netherlands, 1 edition.

Maxwell, J. C. (1865). Viii. a dynamical theory of the electromagnetic field. *Philosophical transactions of the Royal Society of London*, (155):459–512.

Milgram, S., Bickman, L., and Berkowitz, L. (1969). Note on the drawing power of crowds of different size. *Journal of personality and social psychology*, 13(2):79.

Salucci, M., Poli, L., Rocca, P., and Massa, A. (2022). Learned global optimization for inverse scattering problems: Matching global search with computational efficiency. *IEEE Transactions on Antennas and Propagation*, 70(8):6240–6255.

Shung-Wu Lee, Boersma, J., Chak-Lam Law, and Deschamps, G. (1980). Singularity in green's function and its numerical evaluation. *IEEE Transactions on Antennas and Propagation*, 28(3):311–317.

Van Bladel, J. (1961). Some remarks on green's dyadic for infinite space. *IRE Transactions on Antennas and Propagation*, 9(6):563–566.

Van Dyke, M. C. C., Teixeira, M. M., and Barker, B. M. (2019). Fantastic yeasts and where to find them: the hidden diversity of dimorphic fungal pathogens. *Current opinion in microbiology*, 52:55–63.

Yaghjian, A. D. (1980). Electric dyadic green's functions in the source region. *Proceedings of the IEEE*, 68(2):248–263.

Zhang, Y., Yin, T., Zhao, Z., Nie, Z., and Chen, X. (2022). An iterative domain decomposition technique based on subspace-based optimization method for solving highly nonlinear inverse problem. *IEEE Transactions on Geoscience and Remote Sensing*, 60:1–13.

Apêndice A

Como fazer citações

Você pode fazer uma citação de diversas formas. Se você quiser fazer uma citação entre parênteses, você pode fazer assim: (Milgram et al., 1969). Se você quiser mencionar o número da página, você pode fazer assim: (Deb et al., 2002, p. 10). Agora, se você quiser fazer uma citação onde o autor é parte da sentença, você pode fazer assim: Maxwell (1865) afirma que... Se você quiser fazer uma citação com mais de um autor, você pode fazer assim: (Maxwell, 1865; Van Dyke et al., 2019).

Apêndice B

Como escrever equações

Um exemplo básico de equação:

$$\mathscr{F}(\mathbf{r},t) = \mathfrak{Re}\{\mathbf{F}(\mathbf{r})e^{j\omega t}\} \tag{B.1}$$

Um exemplo sobre como escrever múltiplas equações e o uso de fonte cursiva nas letras:

$$\begin{aligned}
\nabla \times \mathscr{E}(\mathbf{r},t) &= -\frac{\partial \mathscr{B}}{\partial t}(\mathbf{r},t) && \text{(B.2)}\\
\nabla \times \mathscr{H}(\mathbf{r},t) &= \frac{\partial \mathscr{D}}{\partial t}(\mathbf{r},t) + \mathscr{J}(\mathbf{r},t) && \text{(B.3)}\\
\nabla \cdot \mathscr{D}(\mathbf{r},t) &= \rho(\mathbf{r},t) && \text{(B.4)}\\
\nabla \cdot \mathscr{B}(\mathbf{r},t) &= 0 && \text{(B.5)}
\end{aligned}$$

Um exemplo de desenvolvimento de equação:

$$\begin{aligned}
\nabla \times \mathbf{H}(\mathbf{r}) &= j\omega\varepsilon_0\varepsilon_r\mathbf{E}(\mathbf{r}) + \sigma(\mathbf{r})\mathbf{E}(\mathbf{r}) + \mathbf{J}_i(\mathbf{r}) && \text{(B.6)}\\
&= j\omega\varepsilon_0\left(\varepsilon_r(\mathbf{r}) - j\frac{\sigma(\mathbf{r})}{\omega\varepsilon_0}\right)\mathbf{E}(\mathbf{r}) + \mathbf{J}_i(\mathbf{r}) && \text{(B.7)}\\
&= j\omega\varepsilon(\mathbf{r})\mathbf{E}(\mathbf{r}) + \mathbf{J}_i(\mathbf{r}) && \text{(B.8)}
\end{aligned}$$

Um exemplo de equação quebrada em mais de uma linha:

$$\begin{aligned}
\chi(\boldsymbol{\rho})E_{z_i}(\boldsymbol{\rho}) = J_{z_{eq}}(\boldsymbol{\rho}) + \frac{jk_b^2}{4}\chi(\boldsymbol{\rho})\int_S dS' J_0(k_b|\boldsymbol{\rho}-\boldsymbol{\rho}'|)J_{z_{eq}}(\boldsymbol{\rho}')&\\
+\frac{jk_b^2}{4}\chi(\boldsymbol{\rho})\int_S dS' Y_0(k_b|\boldsymbol{\rho}-\boldsymbol{\rho}'|)J_{z_{eq}}(\boldsymbol{\rho}')& \quad \text{(B.9)}
\end{aligned}$$

Um exemplo de equação com somatórios e integrais:

$$\begin{aligned}
\iint_D E_{z_s}(\theta,\phi) w_u^{(\theta)}(\theta) w_v^{(\phi)}(\phi) d\theta d\phi = \\
-\frac{jk_b^2}{4} \sum_{i=1}^{N_I} \sum_{j=1}^{N_J} \sum_{p=1}^{N_P} \sum_{q=1}^{N_Q} \sum_{r=1}^{N_R} a_{ij} b_{pqr} \iint\limits_D \iint\limits_S d\theta d\phi dx dy \Big[G_{2D}^D(\theta,x,y) \\
f_i^{(x)}(x) f_j^{(y)}(y) g_p^{(x)}(x) g_q^{(y)}(y) g_r^{(\phi)}(\phi) w_u^{(\theta)}(\theta) w_v^{(\phi)}(\phi) \Big], \\
u = 1, \cdots, N_U,\ v = 1, \cdots, N_V
\end{aligned} \tag{B.10}$$

Um exemplo de definição de matriz:

$$\bar{\mathbf{\Lambda}} = \begin{bmatrix} \Lambda_{11} & \Lambda_{12} & \cdots & \Lambda_{1N_V} \\ \Lambda_{21} & \Lambda_{22} & \cdots & \Lambda_{2N_V} \\ \vdots & \vdots & \vdots & \vdots \\ \Lambda_{u1} & \Lambda_{u2} & \cdots & \Lambda_{uN_V} \\ \vdots & \vdots & \vdots & \vdots \\ \Lambda_{N_U 1} & \Lambda_{N_U 2} & \cdots & \Lambda_{N_U N_V} \end{bmatrix} \tag{B.11}$$

Um exemplo de definição de casos:

$$w_{uv} = \begin{cases} 1, & \text{in } D_{uv}, \\ 0, & \text{outside, } D_{uv} \end{cases} \tag{B.12}$$

Um exemplo para organização de três matrizes em uma mesma linha:

$$\bar{\boldsymbol{\chi}} = \begin{bmatrix} \chi_{11} & 0 & \cdots & 0 \\ 0 & \chi_{12} & \cdots & 0 \\ \vdots & \vdots & \ddots & \vdots \\ 0 & 0 & \cdots & \chi_{N_I N_J} \end{bmatrix} \quad \bar{\boldsymbol{\beta}} = \begin{bmatrix} \beta_{11} & 0 & \cdots & 0 \\ 0 & \beta_{12} & \cdots & 0 \\ \vdots & \vdots & \ddots & \vdots \\ 0 & 0 & \cdots & \beta_{N_I N_J} \end{bmatrix} \quad \bar{\mathbf{R}} = \begin{bmatrix} R_{11} & 0 & \cdots & 0 \\ 0 & R_{12} & \cdots & 0 \\ \vdots & \vdots & \ddots & \vdots \\ 0 & 0 & \cdots & R_{N_I N_J} \end{bmatrix} \tag{B.13}$$

Note que você pode referenciar equações das seguintes formas:

- Quando ela estiver no meio da frase, você pode usar simplesmente o comando `\eqref{}`. Por exemplo: "...como mostrado em (B.2), ..."
- Quando você estiver no início da frase, você pode escrever: "A Eq. (B.2) mostra que..."

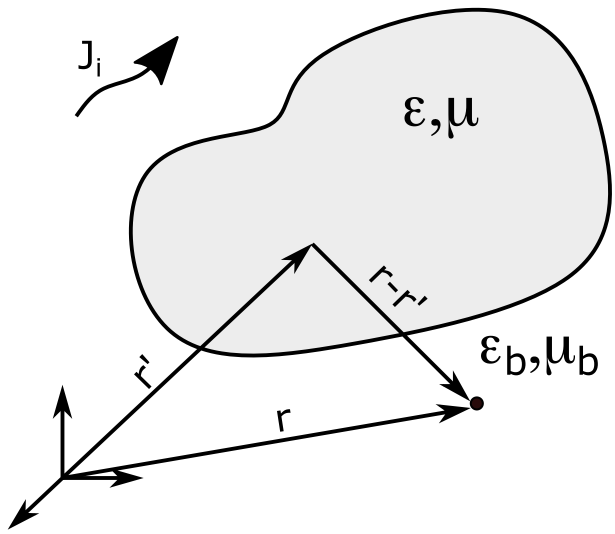

Figura C.1: General scattering problem.

Apêndice C

Como inserir figuras

Um exemplo sobre como inserir figuras simples pode ser visto em C.1. Você pode referenciar figuras através do comando `\ref{}` ou do comando `\autoref{}`. O primeiro comando apenas referencia o número da figura, enquanto o segundo comando referencia o número da figura e o nome dela. Por exemplo, você pode escrever: “...como mostrado na Figura C.1, ...”.

Um exemplo de múltiplas figuras pode ser visto na Figura C.2.

Um outro exemplode múltiplas figuras pode ser visto na Figura C.3.

Exemplo para inserir duas figuras horizontais C.4:

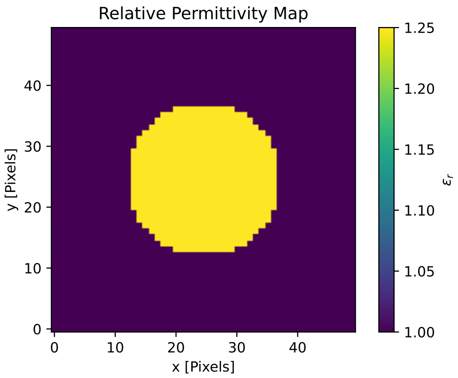

(a)

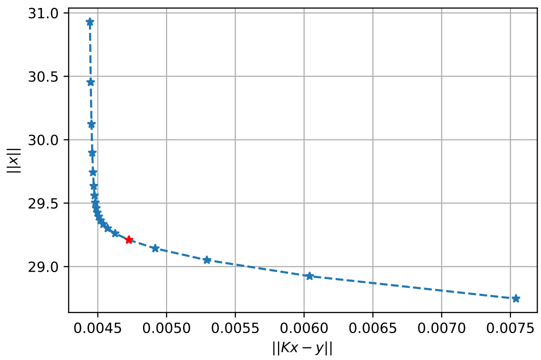

(b)

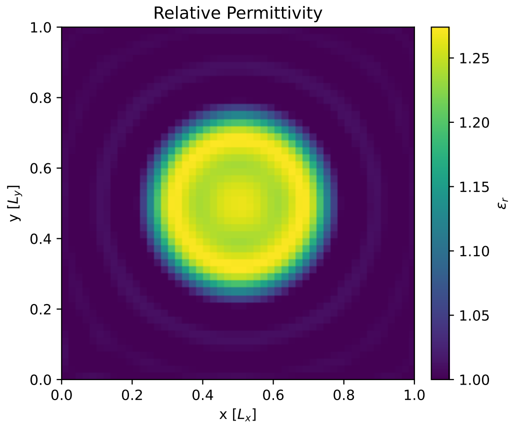

(c)

Figura C.2: Example of applying the L-curve Method to a linear problem where it presupposes knowledge of the total field. (a) A simple instance of a contrast dielectric circle $\chi = 0.25$ and radius $0.8\lambda_b$. Respecting the degrees of freedom, the scattered field was sampled in 45 positions for 45 incidence angles at a distance of $10\lambda_b$ from the center of the image. (b) L-curve considering 20 values of α_T in a range of 10^{-5} a 10^{-2}. The red dot represents the solution with the shortest normalized distance to the origin. Its α_T value is approximately 2.3357×10^{-3}. (c) Reconstruction of the image using the α_T value from the red dot. No inverse crime was committed since the data were obtained from the analytical solution.

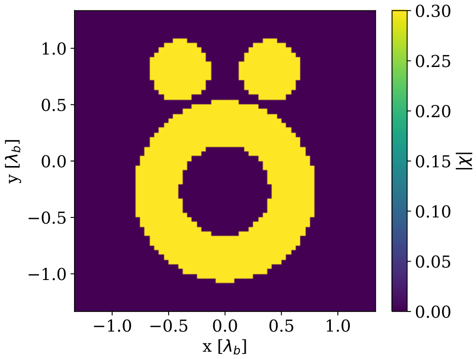

(a)

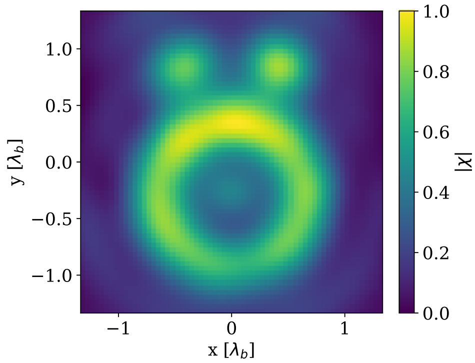

(b)

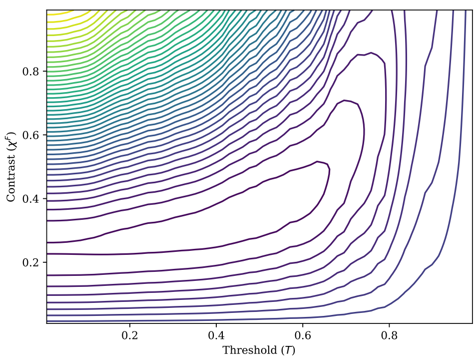

(c)

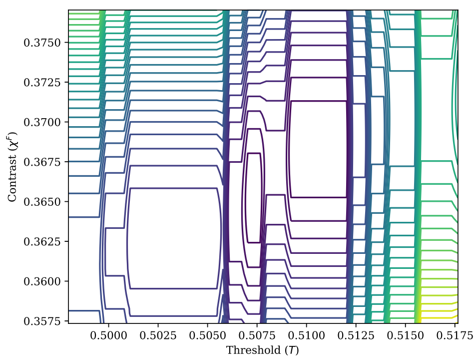

(d)

Figura C.3: Example of an objective function resulting from the transformation of the inversion problem into a two-dimensional optimization one: (a) the ground-truth image; (b) the image obtained by OSM; (c) the surface obtained by the transformation of the inversion problem into a two-dimensional optimization one; and (d) a zoom over the region close to the optimum.

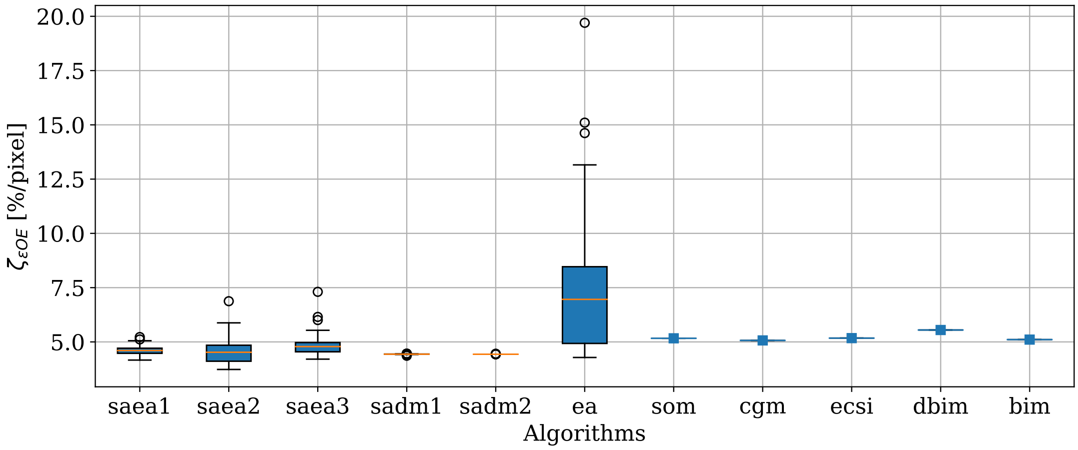

(a)

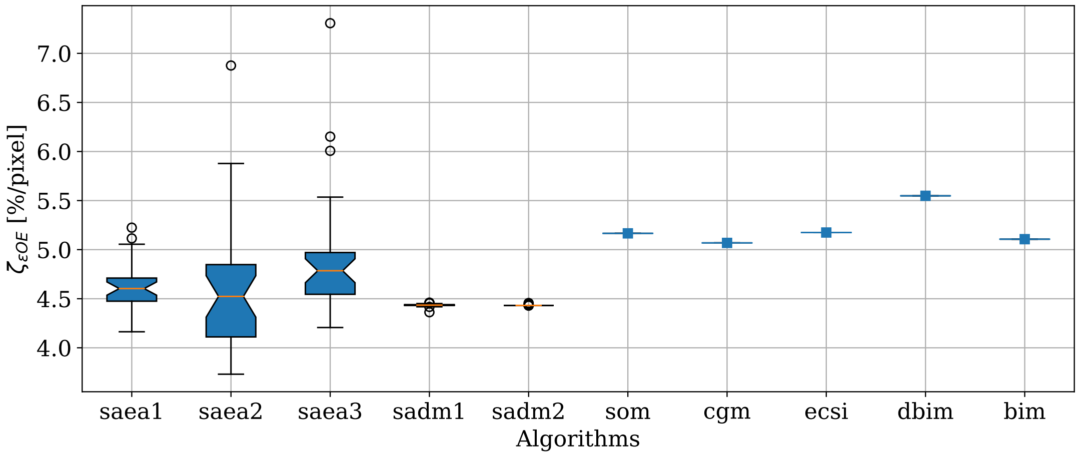

(b)

Figura C.4: Performance of $\zeta_{\varepsilon OE}$ indicator for various algorithms in the Austria profile. (a) Boxplots show quartiles of 30 executions for stochastic algorithms, and the solid line represents the deterministic algorithms. (b) Exclusion of the EA algorithm for better visualization of differences among algorithms.

Apêndice D

Como inserir tabelas

Um exemplo de tabela simples é a D.1.

Tabela D.1: Parameters for problem specification of Austria profile case study.

N_M	N_S	R_O	f	L_X, L_Y	ε_{rb}
32	16	6 [m]	400 [MHz]	2 [m]	1

Um exemplo de tabela simples pode ser visto em D.2. Você pode referenciar tabelas da mesma forma que você referencia figuras. Por exemplo, você pode escrever: “...como mostrado na Tabela D.2, ...”.

Exemplo de tabelas em landscape:

Tabela D.2: Classification of methods by their properties.

Classes	Methods			
Qualitative	Linear Sampling Method			
	Orthogonality Sampling Method			
Quantitative	Deterministic	Linear	Born Approximation	
			Rytov Approximation	
			Back-Propagation Method	
			Dominant Current Scheme	
		Nonlinear	Forward and inverse subproblems	Born Iterative Method
				Distorted Born Iterative Method
				Variational Born Iterative Method
				Level-Set Method
			Gradient-based	Conjugated-Gradient Method
				Contrast Source Inversion
				Subspace-based Optimization Method
			Other	Compressive Sensing
				Regularization on Lp Banach Spaces
				Virtual Experiments
				Deep learning methods
	Stochatisc	Components	Types	
		Representation	Known geometries	
			Contours	
			Pixel-based	
		Objective function	Data equation residual	
			Data and state equation residual	

Tabela D.3: P-values for posthoc multiple pairwise comparisons considering the $\zeta_{\varepsilon OE}$ indicator, with the compatible statistical test for each test set. The significance level has been corrected using the Bonferroni method, resulting in 0.0083. Detected differences are indicated in bold format. Confidence intervals are compute for means when Paired T-Test are evaluated and for medians when the Wilcoxon Signed-Rank Test is evaluated.

Pairs	$\chi = 0.5$ Wilcoxon Signed-Rank test		$\chi = 1$ Paired T-Test		$\chi = 2$ Wilcoxon Signed-Rank test		$\chi = 3$ Wilcoxon Signed-Rank test	
	p-value	Confi. In.	p-value	Confi. In.	p-value	Confi. In.	p-value	Confi. In.
SAEA1-SAEA2	0.2988	(-0.031, 0.034)	**<0.0001**	(0.322, 0.895)	**<0.0001**	(0.675, 1.576)	**<0.0001**	(0.4, 1.484)
SAEA1-SAEA3	0.1706	(0.012, 0.124)	**<0.0001**	(-2.5, -1.33)	**<0.0001**	(-2.165, -0.916)	**<0.0001**	(-2.574, -1.019)
SAEA1-SADM2	0.0577	(-0.089, 0.002)	**0.003**	(-1.99, -0.132)	0.6702	(-0.804, 0.842)	0.2054	(-1.35, 0.862)
SAEA2-SAEA3	0.2988	(-0.017, 0.148)	**<0.0001**	(-3.18, -1.87)	**<0.0001**	(-4.152, -2.3)	**<0.0001**	(-4.301, -2.237)
SAEA2-SADM2	0.0164	(-0.109, -0.009)	**<0.0001**	(-2.71, -0.634)	**0.0008**	(-1.542, -0.063)	**0.0015**	(-2.494, 0.137)
SAEA3-SADM2	0.1347	(-0.21, -0.023)	0.023	(-0.153, 1.86)	0.0113	(0.912, 3.128)	0.1642	(-0.886, 2.103)

Tabela D.4: P-values for posthoc multiple pairwise comparisons obtained by Wilcoxon Signed-Rank tests considering the ζ_S indicator. The significance level has been corrected using the Bonferroni method, resulting in 0.0083. Detected differences are indicated in bold format. The confidence interval for medians is also presented.

Pairs	$\chi = 0.5$		$\chi = 1$		$\chi = 2$		$\chi = 3$		$\chi = 4$	
	p-value	Confi. In.	p-value	Confi. In.	p-value	Confi. In.	p-value	Confi. In.	p-value	Confi. In.
SAEA1-SAEA2	**<0.0001**	(0.34, 0.92)	**<0.0001**	(0.49, 1.09)	**<0.0001**	(1.02, 2.04)	**0.0002**	(0.67, 2.01)	0.0145	(0.2, 2)
SAEA1-SAEA3	**0.0002**	(-1.32, -0.49)	**<0.0001**	(-5.38, -3.52)	**<0.0001**	(-2.46, -1.34)	**<0.0001**	(-3.16, -1.28)	**0.0066**	(-3.08, -0.92)
SAEA1-SADM2	**0.0012**	(0.02, 0.69)	**0.0081**	(-2.38, 0.37)	0.3931	(-0.85, 0.59)	0.1706	(-1.72, 1.16)	0.9515	(-1.70, 1.58)
SAEA2-SAEA3	**<0.0001**	(-2.15, -0.97)	**<0.0001**	(-5.80, -3.40)	**<0.0001**	(-4.69, -1.97)	**<0.0001**	(-5.73, -2.71)	**0.0028**	(-4.79, -1.37)
SAEA2-SADM2	0.1996	(-0.20, 0.15)	**<0.0001**	(-2.64, -0.17)	**<0.0001**	(-2.70, -0.66)	**0.0007**	(-3.61, 0.08)	0.1059	(-2.17, 0.72)
SAEA3-SADM2	**<0.0001**	(0.51, 1.82)	**0.0081**	(0.91, 3.32)	0.0087	(0.83, 2.88)	0.2801	(-0.62, 1.93)	0.1094	(0.67, 4.32)

Apêndice E

Como inserir algoritmos

Um exemplo de algoritmo é o seguinte:

Algorithm 1: Distorted Born Iterative Method.

Input: $\bar{\mathbf{E}}^{\mathbf{s}}, \bar{\mathbf{G}}^{\mathbf{2D}}, \bar{\mathbf{G}}^{\mathbf{S}}$
Output: $\bar{\boldsymbol{\chi}}, \bar{\mathbf{E}}$
Compute an initial guess $\bar{\boldsymbol{\chi}}^{\mathbf{0}}$ based on available information
$t \leftarrow 0$
while *some criterion is not reached* **do**
    Solve $\left(\bar{\mathbf{I}} - \bar{\mathbf{G}}^{\mathbf{S}} \bar{\boldsymbol{\chi}}^{t}\right) \bar{\mathbf{G}}^{\mathbf{in},t} = \bar{\mathbf{G}}^{\mathbf{2D}}$ for $\bar{\mathbf{G}}^{\mathbf{in},t}$
    Solve the direct problem for $\bar{\mathbf{E}}^{t}$ and $\bar{\mathbf{E}}^{\mathbf{s},t}$
    $\Delta\bar{\mathbf{E}}^{\mathbf{s}} = \bar{\mathbf{E}}^{s} - \bar{\mathbf{E}}^{\mathbf{s},t}$
    Solve the inverse linear problem $\Delta\bar{\mathbf{E}}^{\mathbf{s}} = \bar{\mathbf{G}}^{\mathbf{in},t} \Delta\bar{\boldsymbol{\chi}} \bar{\mathbf{E}}^{t}$ for $\Delta\bar{\boldsymbol{\chi}}$
    $\bar{\boldsymbol{\chi}}^{t} \leftarrow \bar{\boldsymbol{\chi}}^{t-1} + \Delta\bar{\boldsymbol{\chi}}^{t}$
    $t \leftarrow t+1$
end

Apêndice F

Como inserir definições e outras coisas especiais

Um exemplo de definição:

Definição 1. *Projection Operator*
Let X be a normed space over the field $\mathbb{K} = \mathbb{R}$ or $\mathbb{K} = \mathbb{C}$. Let $U \subset X$ be a closed subspace. A linear bounded operator $\mathscr{P} : X \to X$ is called a projection operator on U if

- $\mathscr{P}\{x\} \in U$, $\forall x \in X$ *and*
- $\mathscr{P}\{x\} = x$, $\forall x \in U$.

Apêndice G

Dyadic Green's Function

The dyadic Green's function is an important tool for solving electromagnetic problems that include the radiation phenomenon. For this reason, this appendix aims to briefly discuss its definition and singularity. This text is based on chapter 7 of the book written by Chew (1995), which deepens the discussion and provides a better bibliographical reference on the topic.

G.1 Dyadic Green's Function for Homogeneous Medium

A very general and essential problem for electromagnetic theory is that of radiation from a point source. This problem is fundamental for integral equations since the radiation of a current distribution is based on the contribution of all points at which the current is defined. That is, considering a generic scalar problem such as:

$$(\nabla^2 + k^2)\phi(\mathbf{r}) = s(\mathbf{r}) \tag{G.1}$$

defined in a homogeneous region V, the solution can be obtained through:

$$\psi(\mathbf{r}) = -\int_V d\mathbf{r}' g(\mathbf{r},\mathbf{r}')s(\mathbf{r}') \tag{G.2}$$

where $g(\mathbf{r},\mathbf{r}')$ is the Green's function which is the solution to the equation:

$$(\nabla^2 + k^2)g(\mathbf{r},\mathbf{r}') = -\delta(\mathbf{r}-\mathbf{r}') \tag{G.3}$$

Particularly, this solution follows from the interpretation that $s(\mathbf{r})$ is a linear superposition of point sources.

To obtain Green's function for a homogeneous and infinite medium, we will change the source position in the problem of eq.(G.3) to the origin of spherical coordinates:

$$(\nabla^2 + k^2)g(\mathbf{r}) = -\delta(\mathbf{r}) = -\delta(x)\delta(y)\delta(z) \tag{G.4}$$

For $\mathbf{r} \neq 0$, the solution of (G.4) is given by:

$$g(\mathbf{r}) = C\frac{e^{jkr}}{r} + D\frac{e^{-jkr}}{r} \tag{G.5}$$

where $r = |\mathbf{r}|$. Assuming that there are no sources at infinity, only the first term on the right-hand side of (G.5) is a solution:

$$g(\mathbf{r}) = C\frac{e^{jkr}}{r} \tag{G.6}$$

The constant C is determined by calculating both sides of (G.4) in the singularity. To do this, we combine (G.6) into (G.4) and integrated into a small volume around the origin:

$$\int_{\Delta V} dV \nabla \cdot \nabla \frac{Ce^{jkr}}{r} + \int_{\Delta V} dV k^2 \frac{Ce^{jkr}}{r} = -1 \tag{G.7}$$

The second integral of (G.7) tends to zero if $\Delta V \to 0$, since $dV = 4\pi r^2 dr$. Besides, Gauss' theorem can be used to transform the first integral into a surface one, and with that, we obtain:

$$\lim_{r\to 0} 4\pi r^2 \frac{d}{dr} C\frac{e^{jkr}}{r} = -1 \tag{G.8}$$

or $C = 1/4\pi$. Also, the solution (G.6) can be generalized for the case in which the source is shifted to a point $\mathbf{r}'$. In this case, eq.(G.6) can be rewritten as:

$$g(\mathbf{r},\mathbf{r}') = g(\mathbf{r}-\mathbf{r}') = \frac{e^{jk|\mathbf{r}-\mathbf{r}'|}}{4\pi|\mathbf{r}-\mathbf{r}'|} \tag{G.9}$$

Solution (32) can be used to obtain Green's dyadic[1] function for the vector wave equation in a homogeneous and isotropic medium:

$$\nabla \times \nabla \times \mathbf{E}(\mathbf{r}) - k^2\mathbf{E}(\mathbf{r}) = -j\omega\mu\mathbf{J}(\mathbf{r}) \tag{G.10}$$

Since $\nabla \times \nabla \times \mathbf{E} = -\nabla^2\mathbf{E} + \nabla\nabla \cdot \mathbf{E}$ and that, according to the continuity equation, $\nabla \cdot \mathbf{E} = \rho/\varepsilon = \nabla \cdot \mathbf{J}/j\omega\varepsilon$, eq.(G.10) can be rewritten as:

$$\nabla^2\mathbf{E}(\mathbf{r}) + k^2\mathbf{E}(\mathbf{r}) = j\omega\mu \left[\bar{\mathbf{I}} + \frac{\nabla\nabla}{k^2}\right] \cdot \mathbf{J}(\mathbf{r}) \tag{G.11}$$

where $\bar{\mathbf{I}}$ is the identity operator. In Cartesian coordinates, eq.(G.11) is actually three equations that can be solved just as it was done for the scalar equation. Thus, the solution for (G.11) is:

$$\mathbf{E}(\mathbf{r}) = -j\omega\mu \int_V d\mathbf{r}' g(\mathbf{r}'-\mathbf{r}) \left[\bar{\mathbf{I}} + \frac{\nabla'\nabla'}{k^2}\right] \cdot \mathbf{J}(\mathbf{r}') \tag{G.12}$$

[1]Dyad is an example of a second rank tensor, formed from two vectors and maps one vector field to another. Besides, they have the property of having nullspace of rank two. For a deeper discussion of tensors and their mathematical properties, we recommend reading Appendix B of (Chew, 1995).

Taking into account the vector identities $\nabla gf = f\nabla g + g\nabla f$ and $\nabla \cdot g\mathbf{F} = g\nabla\cdot\mathbf{F} + (\nabla g)\cdot\mathbf{F}$, the following integrals can be rewritten as:

$$\int_V d\mathbf{r}' g(\mathbf{r}'-\mathbf{r})\nabla' f(\mathbf{r}') = -\int_V \left[\nabla' g(\mathbf{r}'-\mathbf{r})\right] f(\mathbf{r}') \tag{G.13}$$

$$\int_V d\mathbf{r}' \left[\nabla' g(\mathbf{r}'-\mathbf{r})\right] \nabla'\cdot\mathbf{J}(\mathbf{r}') = -\int_V d\mathbf{r}'\mathbf{J}(\mathbf{r}')\cdot\nabla'\nabla' g(\mathbf{r}'-\mathbf{r}) \tag{G.14}$$

which allows us to rewrite (G.12) as:

$$\mathbf{E}(\mathbf{r}) = -j\omega\mu \int_V d\mathbf{r}'\mathbf{J}(\mathbf{r}')\cdot\left[\bar{\mathbf{I}} + \frac{\nabla'\nabla'}{k^2}\right] g(\mathbf{r}',\mathbf{r}) \tag{G.15}$$

However, as demonstrated in chapter 7 of (Chew, 1995), it is also possible to write eq.(G.15) as follows:

$$\mathbf{E}(\mathbf{r}) = j\omega\mu \int_V d\mathbf{r}'\mathbf{J}(\mathbf{r}')\cdot\bar{\mathbf{G}}(\mathbf{r},\mathbf{r}') \tag{G.16}$$

where:

$$\bar{\mathbf{G}}(\mathbf{r},\mathbf{r}') = -\left[\bar{\mathbf{I}} + \frac{\nabla\nabla}{k^2}\right]\frac{e^{jk|\mathbf{r}-\mathbf{r}'|}}{4\pi|\mathbf{r}-\mathbf{r}'|} \tag{G.17}$$

G.2 The Singularity of the Dyadic Green's Function

As can be seen in equation (G.13), Green's dyadic function has singularity for $\mathbf{r}=\mathbf{r}'$. That is, to calculate the field at a point within the region of the source $\mathbf{J}$, it is necessary to rewrite the integral equation (G.16) with the support of the exclusion volume V_δ around the singularity point:

$$\mathbf{E}(\mathbf{r}) = \lim_{V_\delta\to 0} j\omega\mu \int\limits_{V-V_\delta} d\mathbf{r}'\mathbf{J}(\mathbf{r}')\cdot\bar{\mathbf{G}}(\mathbf{r}',\mathbf{r}) \tag{G.18}$$

In this way, the equation is defined in terms of an improper integral. Generally, improper integrals converge if there is a fixed limit regardless the shape of V_δ. However, in the case of (G.18), a necessary condition for convergence is that $\mathbf{J}$ must satisfy Holder's condition (Kellogg, 1953) in $\mathbf{r}=\mathbf{r}'$, in which there must be constants c, A, and α such that $|\mathbf{J}(\mathbf{r})-\mathbf{J}(\mathbf{r}')\leq A|\mathbf{r}'-\mathbf{r}|^\alpha$ for $|\mathbf{r}'-\mathbf{r}|<c$. This condition is slightly stronger than general continuity. In addition, the derivatives of (G.17) do not allow the integral to converge in a traditional fashion, i.e., the principal value of the integral exists but depends on the chosen shape for V_δ.

To calculate the limit of the term that includes those derived in eq.(G.18), we need to take into account both the integral over the region without the singularity and the region with the singularity:

$$\nabla\nabla\cdot\int_V d\mathbf{r}' g(\mathbf{r},\mathbf{r}')\mathbf{J}(\mathbf{r}') = \lim_{V_\delta\to 0}\left[\nabla\nabla\cdot\int\limits_{V-V_\delta} d\mathbf{r}' g(\mathbf{r},\mathbf{r}')\mathbf{J}(\mathbf{r}') + \nabla\nabla\cdot\int\limits_{V_\delta} d\mathbf{r}' g(\mathbf{r},\mathbf{r}')\mathbf{J}(\mathbf{r}')\right] \tag{G.19}$$

where $\mathbf{r}\in V_\delta$. The first integral on the right-hand side of the equation does not contain $\mathbf{r}$, so the operator $\nabla\nabla\cdot$ might enter into the integral. The second integral converges only if an operator ∇ is introduced in the integral. In this way, eq.(G.19) can be rewritten as:

$$\nabla\nabla\cdot\int_V d\mathbf{r}' g(\mathbf{r},\mathbf{r}')\mathbf{J}(\mathbf{r}') = \lim_{V_\delta\to 0}\left[\int\limits_{V-V_\delta} d\mathbf{r}'\nabla\nabla\cdot g(\mathbf{r},\mathbf{r}')\mathbf{J}(\mathbf{r}') - \nabla\int\limits_{V_\delta} d\mathbf{r}'\nabla' g(\mathbf{r},\mathbf{r}')\cdot\mathbf{J}(\mathbf{r}')\right] \tag{G.20}$$

Therefore, the two integrals on the right-hand side of (G.20) converge to a value that depends on the shape of V_δ. However, the sum of the two integrals must be equal to the left-hand side, which does not depend on the shape chosen for V_δ.

If we use the integration by parts and the relation $\nabla\cdot\mathbf{J} = j\omega\rho$, the second integral of (46) can be rewritten as:

$$\nabla\int\limits_{V_\delta} d\mathbf{r}'\nabla' g(\mathbf{r},\mathbf{r}')\cdot\mathbf{J}(\mathbf{r}') = \int_{S_\delta} dS'\mathbf{n}\cdot\mathbf{J}(\mathbf{r}')g(\mathbf{r},\mathbf{r}') - j\omega\int_{V_\delta} g(\mathbf{r},\mathbf{r}')\rho(\mathbf{r}') \tag{G.21}$$

The second integral of (G.21) will tend to zero when $V_\delta\to 0$ assuming that, for a volumetric current, $\rho(\mathbf{r})$ is continuous. The first integral, on the other hand, has the term $\mathbf{n}\cdot\mathbf{J}(\mathbf{r}')$ which is the surface charge on S_δ, the surface of V_δ. Because of this surface charge, the first integral is proportional to the field in $\mathbf{r}$ and does not vary depending on the scale. In other words, it does not disappear when $V_\delta\to 0$, but depends on the shape of V_δ. At the limit, eq.(G.21) is linearly proportional to $\mathbf{J}(\mathbf{r})$. Therefore, with the aid of $\bar{\mathbf{L}}$, a dyad which depends on the shape of V_δ, we can rewrite (G.20) as:

$$\nabla\nabla\cdot\int_V d\mathbf{r}' g(\mathbf{r},\mathbf{r}')\mathbf{J}(\mathbf{r}') = \lim_{V_\delta\to 0}\int\limits_{V-V_\delta} d\mathbf{r}'\nabla\nabla(\mathbf{r},\mathbf{r}')\cdot\mathbf{J}(\mathbf{r}') - \bar{\mathbf{L}}\cdot\mathbf{J}(\mathbf{r}) \tag{G.22}$$

Using this result in (G.16), we will obtain:

$$\mathbf{E}(\mathbf{r}) = j\omega\mu \lim_{V_\delta \to 0} \int\limits_{V-V_\delta} d\mathbf{r}'\bar{\mathbf{G}}(\mathbf{r},\mathbf{r}')\cdot\mathbf{J}(\mathbf{r}') + \frac{\bar{\mathbf{L}}\cdot\mathbf{J}(\mathbf{r})}{j\omega\varepsilon} \tag{G.23}$$

The integral of (G.23) is equivalent to the principal value integral operator whose notation is expressed by $P.V. \int_V$, that is:

$$\mathbf{E}(\mathbf{r}) = j\omega\mu P.V. \int_V d\mathbf{r}'\bar{\mathbf{G}}(\mathbf{r},\mathbf{r}')\cdot\mathbf{J}(\mathbf{r}') + \frac{\bar{\mathbf{L}}\cdot\mathbf{J}(\mathbf{r})}{j\omega\varepsilon}, \quad \forall\mathbf{r}\in V \tag{G.24}$$

Therefore, although the two terms on the right-hand side of (G.24) are dependent on the choice of V_δ, the $\mathbf{E}$ field is unique. This method for determining the field value in the region of singularity is known as the Principal Volume Method (Van Bladel, 1961).

Physically, this method of solution corresponds to opening a space around the observation point within the current region. Since this current is discontinuous on the surface of that space, the surface accumulates charges which, when decreasing the space to an infinitesimal volume, have an electrostatic nature. This electrostatic field satisfies the Laplace equation and depends on the shape of that space, no matter how small it is. Therefore, the second term in eq.(G.24) aims to remove the contribution from this electrostatic field, since it is not part of the problem but has been added as a mathematical resource.

Finally, some values for $\bar{\mathbf{L}}$ for certain types of exclusion volumes have already been determined in the literature (Shung-Wu Lee et al., 1980; Yaghjian, 1980). In addition, generally, the trace $\left[\bar{\mathbf{L}}\right] = 1$ (Yaghjian, 1980). Board G.1 shows some values for $\bar{\mathbf{L}}$ considering some geometric shapes:

Tabela G.1: Dyad $\bar{\mathbf{L}}$ values for different shapes of exclusion volume applied to the singularity of dyadic Green's function. Sources: (Shung-Wu Lee et al., 1980; Yaghjian, 1980).

Geometric shape	$\bar{\mathbf{L}}$
Spheres or cubes	$\frac{\bar{\mathbf{I}}}{3}$
Disks	$\mathbf{zz}$
Needles	$\frac{\mathbf{xx}+\mathbf{yy}}{2}$

G.3 Dyadic Green's Function for Inhomogeneous Medium

To determine the dyadic Green function for a non-homogeneous medium, we will assume a region V_1 and another $V_2 \subset V_1$. The contrasts of these media in relation to the vacuum will be denominated χ_1 and χ_2, respectively. We can write χ_2 as:

$$\chi_2(\mathbf{r}) = \chi_1(\mathbf{r}) + \Delta\chi(\mathbf{r}) \tag{G.25}$$

Consequently, the integral equation for the electric field at any point in space can be written as:

$$\mathbf{E}(\mathbf{r}) = \mathbf{E_i}(\mathbf{r}) + k_0^2 \int_{V_1} d\mathbf{r}'\ \bar{\mathbf{G}}(\mathbf{r},\mathbf{r}') \cdot \chi_1(\mathbf{r}')\mathbf{E}(\mathbf{r}') + k_0^2 \int_{V_1} d\mathbf{r}'\ \bar{\mathbf{G}}(\mathbf{r},\mathbf{r}') \cdot \chi_2(\mathbf{r}')\mathbf{E}(\mathbf{r}') \tag{G.26}$$

However, $\mathbf{E}$ can be interpreted as the sum of the scattered field and by χ_1 for $\mathbf{r} \in V_1$. The former is due to the *excess* of contrast in V_2 when the incident field is the field that propagates in an inhomogeneous medium characterized by ε_0 for $\mathbf{r} \notin V_1$. Mathematically, this is equivalent to:

$$\mathbf{E}(\mathbf{r}) = \mathbf{E_1}(\mathbf{r}) + k_0^2 \int_{V_2} d\mathbf{r}'\ \bar{\mathbf{G}}_{\mathbf{in}}(\mathbf{r},\mathbf{r}') \cdot \chi_2(\mathbf{r}')\mathbf{E}(\mathbf{r}') \tag{G.27}$$

where $\mathbf{E_1}$ is given by:

$$\mathbf{E_1}(\mathbf{r}) = \mathbf{E_i}(\mathbf{r}) + k_0^2 \int_{V_1} d\mathbf{r}'\ \bar{\mathbf{G}}(\mathbf{r},\mathbf{r}') \cdot \chi_1(\mathbf{r}')\mathbf{E}(\mathbf{r}') \tag{G.28}$$

and the Green's function for the inhomogeneous medium satisfies:

$$\bar{\mathbf{G}}_{\mathbf{in}}(\mathbf{r},\mathbf{r}') = \bar{\mathbf{G}}(\mathbf{r},\mathbf{r}') + k_0^2 \int_{V_1} d\mathbf{r}''\bar{\mathbf{G}}(\mathbf{r},\mathbf{r}'') \cdot \chi_1(\mathbf{r}'')\bar{\mathbf{G}}_{\mathbf{in}}(\mathbf{r}'',\mathbf{r}') \tag{G.29}$$

Analytical solutions for (G.29) are rarely available. Frequently, when inhomogeneous modeling for Green's function is necessary, numerical methods are employed to estimate this function.

Apêndice H

Integral Equation Formulation

Integral equations are an important method for electromagnetic theory. In this appendix, the derivation of the Electric Field Integral Equation from wave equation and dyadic Green's function will be discussed. The text is based on section 3.4 of (Chew, 2009).

Let us suppose a volume V_{inf} whose surface is S_{inf} in which there is a source J_2 within a region V_2 and another source J_1 for a region V_1 separate from V_2 for a closed surface S (see Figure H.1). Assuming that the medium in V_1 is homogeneous with properties ε_1 and μ_1, the relationship between electric field $\mathbf{E}(\mathbf{r})$ and a current distribution $\mathbf{J}(\mathbf{r})$ representing currents J_1 and J_2 is given by the wave equation:

$$\nabla \times \nabla \times \mathbf{E}(\mathbf{r}) - \omega^2 \varepsilon_1 \mu_1 \mathbf{E}(\mathbf{r}) = -j\omega\mu_1 \mathbf{J}(\mathbf{r}) \tag{H.1}$$

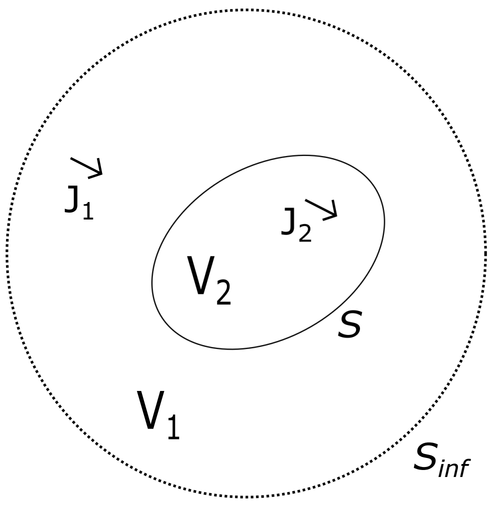

Figura H.1: Derivation of integral equation.

The solution to this equation is obtained with the support of the dyadic Green's function $\bar{\mathbf{G}}(\mathbf{r},\mathbf{r}')$ for a homogeneous and isotropic medium, where $\mathbf{r}'$ is an observation point in the source region. Under these conditions, the Green's function is a solution to the following equation:

$$\nabla \times \nabla \times \bar{\mathbf{G}}(\mathbf{r},\mathbf{r}') - \omega^2 \varepsilon_1 \mu_1 \bar{\mathbf{G}}(\mathbf{r},\mathbf{r}') = -\bar{\mathbf{I}}\delta(\mathbf{r}-\mathbf{r}') \tag{H.2}$$

Postmultiplying (H.1) by $\bar{\mathbf{G}}(\mathbf{r},\mathbf{r}')$, premultiplying (H.2) by $\mathbf{E}(\mathbf{r})$, and then subtracting the resultant equations, we will obtain:

$$\begin{aligned}\mathbf{E}(\mathbf{r}) \cdot \nabla \times \nabla \times \bar{\mathbf{G}}(\mathbf{r},\mathbf{r}') - \nabla \times \nabla \times \mathbf{E}(\mathbf{r}) \cdot \bar{\mathbf{G}}(\mathbf{r},\mathbf{r}') \\ = j\omega\mu_1 \mathbf{J}(\mathbf{r}) \cdot \bar{\mathbf{G}}(\mathbf{r},\mathbf{r}') - \mathbf{E}(\mathbf{r})\delta(\mathbf{r}-\mathbf{r}')\end{aligned} \tag{H.3}$$

If we integrate both sides of the equation (H.3) in the volume V_1, we get:

$$\int_{V_1} dV \left[\mathbf{E}(\mathbf{r}) \cdot \nabla \times \nabla \times \bar{\mathbf{G}}(\mathbf{r},\mathbf{r}') - \nabla \times \nabla \times \mathbf{E}(\mathbf{r}) \cdot \bar{\mathbf{G}}(\mathbf{r},\mathbf{r}')\right] = \mathbf{E}_1(\mathbf{r}') - \mathbf{E}(\mathbf{r}')$$

in which:

$$\mathbf{E}(\mathbf{r}') = \int_{V_1} d\mathbf{r}\; \delta(\mathbf{r}-\mathbf{r}')\mathbf{E}(\mathbf{r}) \tag{H.4}$$

$$\mathbf{E}_1(\mathbf{r}') = j\omega\mu_1 \int_{V_1} d\mathbf{r}\; \mathbf{J}_1(\mathbf{r}) \cdot \mathbf{G}(\mathbf{r},\mathbf{r}') \tag{H.5}$$

The field $\mathbf{E}_1$ is produced by the source $\mathbf{J}_1$ in V_1. Since $\mathbf{J}_2$ is not in V_1, it does not contribute to the integral.

Through the identity:

$$\begin{aligned}-\nabla \cdot \left[\mathbf{E}(\mathbf{r}) \times \nabla \times \bar{\mathbf{G}}(\mathbf{r},\mathbf{r}') + \nabla \times \mathbf{E}(\mathbf{r}\times)\bar{\mathbf{G}}(\mathbf{r},\mathbf{r}')\right] \\ = \mathbf{E}(\mathbf{r}) \cdot \nabla \times \nabla \times \bar{\mathbf{G}}(\mathbf{r},\mathbf{r}') - \nabla \times \nabla \times \mathbf{E}(\mathbf{r}) \cdot \bar{\mathbf{G}}(\mathbf{r},\mathbf{r}')\end{aligned} \tag{H.6}$$

we can apply Gauss' theorem and rewrite eq. (H.4) as:

$$\mathbf{E}_1(\mathbf{r}') - \mathbf{E}(\mathbf{r}') = \oint_{S+S_{inf}} dS\mathbf{n} \cdot \left[\mathbf{E}(\mathbf{r}) \times \nabla \times \bar{\mathbf{G}}(\mathbf{r},\mathbf{r}') + \nabla \times \mathbf{E}(\mathbf{r}) \times \bar{\mathbf{G}}(\mathbf{r},\mathbf{r}')\right] \tag{H.7}$$

$$\begin{aligned}= \oint_{S+S_{inf}} dS \cdot \big[\mathbf{n} \times \mathbf{E}(\mathbf{r}) \cdot \nabla \times \bar{\mathbf{G}}(\mathbf{r},\mathbf{r}') \\ - j\omega\mu_1 \mathbf{n} \times \mathbf{H}(\mathbf{r}) \cdot \bar{\mathbf{G}}(\mathbf{r},\mathbf{r}')\big]\end{aligned} \tag{H.8}$$

where $\mathbf{n}$ is the normal vector on the surface S which points outwards. Depending on the position of $\mathbf{r}'$, we have different results for eq.(H.8):

$$\mathbf{E}_1(\mathbf{r}') - \oint_{S+S_{inf}} dS \left[\mathbf{n} \times \mathbf{E}(\mathbf{r}) \cdot \nabla \times \bar{\mathbf{G}}(\mathbf{r},\mathbf{r}') - j\omega\mu_1 \mathbf{n} \times \mathbf{H}(\mathbf{r}) \cdot \bar{\mathbf{G}}(\mathbf{r},\mathbf{r}')\right] = \begin{cases}\mathbf{E}(\mathbf{r}'), & \mathbf{r}' \in V_1 \\ 0, & \mathbf{r}' \notin V_1\end{cases} \tag{H.9}$$

As the distance between the field observation point and the source point increases, the integral over S_{inf} vanishes. Although the surface of S_{inf} increases with this distance, the two terms on the left-hand side of the eq.(H.9) will cancel each other out so that the integrator decays.

Swapping the observations points $\mathbf{r}$ and $\mathbf{r}'$, we get:

$$\mathbf{E}_1(\mathbf{r}) - \oint_S dS' \left[\mathbf{n}' \times \mathbf{E}(\mathbf{r}') \cdot \nabla' \times \bar{\mathbf{G}}(\mathbf{r}',\mathbf{r}) - j\omega\mu_1 \mathbf{n}' \times \mathbf{H}(\mathbf{r}') \cdot \bar{\mathbf{G}}(\mathbf{r}',\mathbf{r})\right] = \begin{cases} \mathbf{E}(\mathbf{r}), & \mathbf{r} \in V_1 \\ 0, & \mathbf{r} \in V_2 \end{cases} \tag{H.10}$$

From the following transposition properties:

$$\nabla \times \bar{\mathbf{G}}(\mathbf{r},\mathbf{r}') = \left[\nabla' \times \bar{\mathbf{G}}(\mathbf{r}',\mathbf{r})\right]^t \tag{H.11}$$

$$\bar{\mathbf{G}}(\mathbf{r},\mathbf{r}') = \left[\bar{\mathbf{G}}(\mathbf{r}',\mathbf{r})\right]^t \tag{H.12}$$

we can calculate the transpose of eq.(H.10) by:

$$\mathbf{E}_1(\mathbf{r}) - \oint_S dS' \left[\nabla \times \bar{\mathbf{G}}(\mathbf{r}',\mathbf{r}) \cdot \mathbf{n}' \times \mathbf{E}(\mathbf{r}') - j\omega\mu_1 \bar{\mathbf{G}}(\mathbf{r}',\mathbf{r}) \cdot \mathbf{n}' \times \mathbf{H}(\mathbf{r}')\right] = \begin{cases} \mathbf{E}(\mathbf{r}), & \mathbf{r} \in V_1 \\ 0, & \mathbf{r} \in V_2 \end{cases} \tag{H.13}$$

Letting $\mathbf{M}_s(\mathbf{r}') = -\mathbf{n}' \times \mathbf{E}(\mathbf{r}')$ and $\mathbf{J}_s(\mathbf{r}') = \mathbf{n}' \times \mathbf{H}(\mathbf{r}')$, we may write the eq.(H.13) in terms of equivalent surface electric and magnetic currents imposed on the S surface. Thus, the equation becomes:

$$\mathbf{E}_1(\mathbf{r}) + \oint_S dS' \left[\bar{\mathbf{G}}(\mathbf{r}',\mathbf{r}) \cdot \mathbf{M}_s(\mathbf{r}') + j\omega\mu_1 \bar{\mathbf{G}}(\mathbf{r}',\mathbf{r}) \cdot \mathbf{J}_s(\mathbf{r}')\right] = \begin{cases} \mathbf{E}(\mathbf{r}), & \mathbf{r} \in V_1 \\ 0, & \mathbf{r} \in V_2 \end{cases} \tag{H.14}$$

In other words, the field observed at a point in the region V_1 is due to the source $\mathbf{J_1}$ in V_1 and the equivalent currents $\mathbf{M}_s$ and $\mathbf{J}_s$ on the surface of S which has the same effect as $\mathbf{J}_2$. It is also worth noting that (H.14) also applies to other types of equivalent currents, such as induction currents due to the penetration of an incident field in a dielectric material. In these cases, eq.(H.14) can simply be written as:

$$\mathbf{E}(\mathbf{r}) = \mathbf{E}^i(\mathbf{r}) + j\omega\mu \oint_S dS' \bar{\mathbf{G}}(\mathbf{r}',\mathbf{r}) \cdot \mathbf{J}(\mathbf{r}') \tag{H.15}$$

Apêndice I

Functional Analysis

An important issue within the scope of integral equations is functional analysis since it is a problem composed of an operator applied to functions of a vector space. Therefore, this chapter is a brief approach to the concepts of normed spaces and operators which will be a reference for discussions found in the dissertation. This text was written based on Appendix A of (Kirsch, 2011). Therefore, more information can be found in this reference and a more in-depth study can also be found in (Lebedev et al., 1996).

I.1 Normed and Hilbert Spaces

Let us start with some basic definitions:

Definição 2. *Inner Product*
Let X be a vector space defined on $\mathbb{K} = \mathbb{R}$ or $\mathbb{K} = \mathbb{C}$. The scalar product is a mapping

$$\langle \cdot, \cdot \rangle : X \times X \to \mathbb{K}$$

with the following properties:

1. $\langle x+y,z \rangle = \langle x,z \rangle + \langle y,z \rangle,\ \forall x,y,z \in X$;
2. $\langle x,y+z \rangle = \langle x,y \rangle + \langle x,z \rangle,\ \forall x,y,z \in X$;
3. $\langle \alpha x,y \rangle = \alpha \langle x,y \rangle, \forall x,y \in X$ *and* $\alpha \in \mathbb{K}$;
4. $\langle x,y \rangle = \overline{\langle y,x \rangle}, \forall x,y \in X$;
5. $\langle x,x \rangle \in \mathbb{R}$ *and* $\langle x,x \rangle \geq 0, \forall x \in X$;
6. $\langle x,x \rangle > 0$ *if* $x \neq 0$;
7. $\langle x,\alpha y \rangle = \bar{\alpha} \langle x,y \rangle, \forall x,y \in X$ *and* $\alpha \in \mathbb{K}$.

Definição 3. *Pre-Hilbert space*
A vector space X over $\mathbb{K}$ with inner product $\langle \cdot, \cdot \rangle$ is called a pre-Hilbert space over $\mathbb{K}$.

Definição 4. *Norm*

Let X be a vector space over the field $\mathbb{K} = \mathbb{R}$ or $\mathbb{K} = \mathbb{C}$. A norm on X is a mapping

$$||\cdot|| : X \to \mathbb{R}$$

with the following properties:

1. $||x|| > 0, \forall x \in X$ *with* $x \neq 0$;
2. $||\alpha x|| = |\alpha|\ ||x||, \forall x \in X$ *and* $\alpha \in \mathbb{K}$;
3. $||x+y|| \leq ||x|| + ||y||$ *and* $||x-y|| \geq \Big|||x|| - ||y||\Big|, \forall x,y, \in X$ *(Triangle Inequality).*

A vector space X over $\mathbb{K}$ with norm $||\cdot||$ is called normed space over $\mathbb{K}$

Now, the following theorem is introduced:

Teorema 5. *Let X be a pre-Hilbert space. The mapping $||\cdot|| : X \to \mathbb{R}$ defined by*

$$||x|| := \sqrt{\langle x,x \rangle},\ x \in X$$

is a norm. Futhermore:

1. $|(x,y)| \leq ||x||||y||, \forall x,y \in X$ *(Cauchy-Schwarz inequality);*
2. $||x \pm y||^2 = ||x||^2 + ||y||^2 \pm 2\mathfrak{Re}\{\langle x,y \rangle\} \forall x,y \in X$ *(binomial formula);*
3. $||x+y||^2 + ||x-y||^2 = 2||x||^2 + 2||y||^2 \forall x,y \in X$.

An example of a pre-Hilbert space over $\mathbb{R}$ is the space of real or complex continuous functions over the interval $[a,b]$, denoted by $C[a,b]$, whose internal product is:

$$(x,y)_{L^2} := \int_a^b x(t)\overline{y(t)}dt, \quad x,y \in C[a,b] \tag{I.1}$$

and whose norm is Euclidean, i.e.:

$$||x||_{L^2} := \sqrt{\langle x,x \rangle} = \sqrt{\int_a^b |x(t)|^2 dt}, \quad x \in C[a,b] \tag{I.2}$$

When a norm is defined for a vector space, it introduces as well a topology. Based on the norm definition, it is also possible to define open, closed, compact sets, and others features. Firstly, we will introduce the definition of a ball with radius r and center $x \in X$ which will be useful for the next definitions:

$$K(x,r) := \{y \in X : ||y-x|| < r\}, \quad K[x,r] := \{y \in X : ||y-x|| \leq r\}$$

Definição 6. *Let X be a normed space over the field $\mathbb{K} = \mathbb{R}$ or $\mathbb{C}$.*

1. *A subset $M \subset X$ is called bounded if there exists $r > 0$ with $M \subset K(x,r)$. The set $M \subset X$ is called open if for every $x \in M$ there exists $\varepsilon > 0$ such that $K(x,\varepsilon) \subset M$. The set $M \subset X$ is called closed if the complement $X \setminus M$ is open.*
2. *A sequence $(x_k)_k \subset X$ is called bounded if there exists $c > 0$ such that $||x_k|| < c$ for all k. The sequence $(x_k)_k \subset X$ is called convergent if there exist $x \in X$ such that $||x - x_k||$*

converges to zero in $\mathbb{R}$. We denote the limit by $x = \lim_{k\to\infty} x_k$, or we write $x_k \to x$ as $k \to \infty$. The sequence $(x_k)_k \subset X$ is called a Cauchy sequence if for every $\varepsilon > 0$ there exists $N \in \mathbb{N}$ with $||x_m - x_k|| < \varepsilon$ for all $m,k \geq N$.

3. *Let $(x_k)_k \subset X$ be a sequence. $x \in X$ is called an accumulation point if there exists a subsequence $(a_{k_n})_n$ that converges to x.*
4. *A set $M \subset X$ is called compact if every sequence in M has an accumulation point in M.*

A property derived from these concepts is that a set M is closed if and only if the limit of each convergent sequence $(x_k)_k \subset M$ also belongs to M. Furthermore, we call the sets $M^o := \{x \in M :$ there exists $\varepsilon > 0$ with $K(x,\varepsilon) \subset Mt\}$ and $\overline{M} := \{x \in X :$ there exists $(x_k)_k \subset M$ with $x = \lim_{k\to\infty} x_k\}$ interior and closure of M, respectively. In addition, the set $M \subset X$ is said to be dense in X if $\overline{M} = X$.

We can exemplify some of these concepts defined through the set $X = C[0,1]$ on $\mathbb{R}$ and $x_k(t) = t^k$, $t \in [0,1]$, $k \in \mathbb{N}$ with norm $||\cdot||_{L^2}$. In this case, the sequence (x_k) converges to zero. The dependence between topological properties and the definition of the norm of a set is usual; however, this is not the case with finite-dimensional spaces in which the properties are independent.

Teorema 7. *Let X be a finite-dimensional space with norms $||\cdot||_1$ and $||\cdot||_2$. Then both norms are equivalent, i.e., there exist constants $c_2 \geq c_1 > 0$ with*

$$c_1||x||_1 \leq ||x||_2 \leq c_2||x||_1, \ \forall x \in X.$$

Therefore, each ball defined on $||\cdot||_1$ contains a ball defined on $||\cdot||_2$ and vice versa.

Teorema 8. *Let X be a normed space over $\mathbb{K}$ and $M \subset X$ be a subset.*

1. *M is closed if and only if $M = \overline{M}$, and M is open if and only if $M = M^o$.*
2. *If $M \neq X$ is a linear subspace, then $M^o = \emptyset$, and $\overline{M}$ is also a linear subspace.*
3. *In finite-dimensional spaces, every subspace is closed.*
4. *Every compact set is closed and bounded. In finite-dimensional spaces, the reverse is also true (Theorem of Bolzano-Weierstrass): In a finite-dimensional normed space, every closed and bounded set is compact.*

From now on, we can introduce an important concept in functional analysis, which is completeness. This concept is a crucial feature of the set of real numbers, for example.

Definição 9. *Banach Space, Hilbert Space*
A normed space X over $\mathbb{K}$ is called complete or a Banach Space if every Cauchy sequence converges in X. A complete pre-Hilbert space is called a Hilbert space.

The spaces $\mathbb{C}^n$ and $\mathbb{R}^n$ with their canonical inner products are examples of Hilbert spaces. The space $C[a,b]$ with inner product $\langle\cdot,\cdot\rangle_{L^2}$ is not an example. However, any normed or pre-Hilbert space can be "completed", i.e., a smaller Banach or Hilbert space that extends X can be defined. Let us see in the next theorem:

Teorema 10. *Let X be a normed space with norm $||\cdot||_X$. There exist a Banach space $(\tilde{X}, ||\cdot||_{\tilde{X}})$*

and a injective linear operator $\mathscr{J} : X \to \tilde{X}$ *such that*

1. *The range* $J(X) \subset \tilde{X}$ *is dense in* $\tilde{X}$*, and*
2. $||\mathscr{J}\{x\}||_{\tilde{X}} = ||x||_X, \ \forall x \in X$*, i.e.,* $\mathscr{J}$ *preserves the norm.*

Furthermore, $\tilde{X}$ *is uniquely determined in the sense that if* $\tilde{X}$ *is a second space with properties 1 and 2 with respect to a linear injective operator* $\hat{\mathscr{J}}$*, then the operator* $\hat{\mathscr{J}}\mathscr{J}^{-1} : \mathscr{J}(X) \to \hat{\mathscr{J}}(X)$ *has an extension to a norm-preserving isomorphism from* $\tilde{X}$ *onto* $\hat{X}$*. In other words,* $\tilde{X}$ *and* $\hat{X}$ *can be identified.*

For the pre-Hilbert space $(C[a,b], \langle\cdot,\cdot\rangle_{L^2})$ to be complete, it is necessary to make use of Lebesgue's integration theory (Bartle, 1995). From the Lebesgue measure and its definitions of measurability and integrability, the complete space of $(C[a,b], \langle\cdot,\cdot\rangle_{L^2})$ will be denoted as $L^2(a,b)$. For this, we first define the vector space $\mathscr{L}^2(a,b) := \{x : (a,b) \to \mathbb{C} : x$ is measurable and $|x|^2$ integrable$\}$, in which scalar addition and multiplication are defined pointwise in almost everywhere. From this, $\mathscr{L}^2(a,b)$ is a vector space since for $x,y \in \mathscr{L}^2(a,b)$ and $\alpha \in \mathbb{C}$, $x+y$ and αx are also measurable and αx, $x+y \in \mathscr{L}^2(a,b)$. We define a sesquilinear form on $\mathscr{L}^2(a,b)$ by:

$$\langle x,y\rangle := \int_a^b x(t)\overline{y(t)}dt, \quad x,y \in \mathscr{L}^2(a,b) \tag{I.3}$$

However, (I.3) is not an inner product on $\mathscr{L}^(a,b)$ since $\langle x,y\rangle = 0$ only implies that x vanishes almost everywhere, i.e., that $x \in \mathscr{N}$, where $\mathscr{N} := \{x \in \mathscr{L}^2(a,b) : x(t) = 0$ almost everywhere on $(a,b)\}$. Now, we define $L^2(a,b)$ as the factor space

$$L^(a,b) := \mathscr{L}^2(a,b) \setminus \mathscr{N} \tag{I.4}$$

and equip $L^2(a,b)$ with the inner product

$$\langle [x],[y]\rangle_{L^2} := \int_a^b x(t)\overline{y(t)}dt, \quad x \in [x], y \in [y]$$

where $[x],[y] \in L^2(a,b)$ are equivalence classes of functions in $\mathscr{L}^2(a,b)$. From now on, we will write $x \in L^2(a,b)$ instead of $x \in [x] \in L^2(a,b)$. Finally, $L^2(a,b)$ is a Hilbert space and contains $C[a,b]$ as a dense subspace.

I.2 Linear Bounded and Compact Operators

In this section, for all definitions and theorems, we will assume that X and Y are normed spaces and $\mathscr{A} : X \to Y$ is a linear operator.

Definição 11. *Boundedness, Norm of* $\mathscr{A}$

The linear operator $\mathscr{A}$ *is called bounded if there exists* $c > 0$ *such that*

$$||\mathscr{A}\{x\}|| \leq c||x||, \ \forall x \in X.$$

The smallest of theses contants is called the norm of $\mathscr{A}$, i.e.,

$$||\mathscr{A}|| := \sup_{x\neq 0} \frac{||\mathscr{A}\{x\}||}{||x||}.$$

Teorema 12. *The following assertions are equivalent:*

1. *$\mathscr{A}$ is bounded.*
2. *$\mathscr{A}$ is continuous at $x = 0$, i.e, $x_j \to 0$ implies that $\mathscr{A}\{x_j\} \to 0$.*
3. *$\mathscr{A}$ is continuous for every $x \in X$.*

Hence, $\mathscr{L}(X,Y)$ can be understood as all bounded linear mappings from X to Y in which the operator norm is a normed space.

Teorema 13. 1. *Let $k \in L^2((c,d) \times (a,b))$. The operator*

$$\mathscr{A}\{x(t)\} := \int_a^b k(t,s)x(s)ds,\ t \in (c,d),\ x \in L^2(a,b) \tag{I.5}$$

is well-defined, linear, and bounded from $L^2(a,b)$ into $L^2(c,d)$. Furthermore,

$$||\mathscr{A}||_{L^2} \leq \int_c^d \int_a^b |k(t,s)|dsdt.$$

2. *Let k be continuous on $[c,d] \times [a,b]$. Then $\mathscr{A}$ is also well-defined, linear, and bounded from $C[a,b]$ into $C[c,d]$ and*

$$||\mathscr{A}||_\infty = \max_{t\in[c,d]} \int_a^b |k(t,s)|ds.$$

Within the context of integral operators, those whose kernel is weakly singular are also of interest. Mathematically, a kernel k is weakly singular in$[a,b] \times [a,b]$ if k is defined and continuous for every $t,s \in [a,b]$, $t \neq s$, and there is a $c > 0$ and $\alpha \in [0,1)$ such that

$$|k(t,s)| \leq c|t-s|^{-\alpha},\ \forall t,s, \in [a,b], t \neq s.$$

Teorema 14. *Let k be weakly singular on $[a,b]$. Then the integral operator $\mathscr{A}$ defined by* (I.5) *for $[c,d] = [a,b]$, is well-defined and bounded as an operator in $L^2(a,b)$ as well as in $C[a,b]$.*

Another important definition for the study is the adjunct operator:

Teorema 15. *Adjoint Operator*

Let $\mathscr{A} : X \to Y$ be a linear and bounded operator between Hilbert spaces. Then there exists one and only linear bounded operator $\mathscr{A}^* : Y \to X$ with the property

$$\langle \mathscr{A}\{x\}, y\rangle = \langle x, \mathscr{A}^*\{y\}\rangle \quad \forall x \in X, y \in Y.$$

This operator $\mathscr{A}^* : Y \to X$ is called the adjoint operator to $\mathscr{A}$. For $X = Y$, the operator $\mathscr{A}$ is *called self-adjoint if $\mathscr{A}^* = \mathscr{A}$.*

To exemplify the adjunct operators, let $X = L^2(a,b)$, $Y = L^2(c,d)$, and $k \in L^2((c,d) \times (a,b))$. The adjoint operator $\mathscr{A}^*$ of the integral operator

$$\mathscr{A}\{x(t)\} = \int_a^b k(t,s)x(s)ds, \quad t \in (c,d), x \in L^2(a,b)$$

which is given by

$$\mathscr{A}^*\{y(t)\} = \int_c^d \overline{k(s,t)}y(s)ds, \quad t \in (a,b), y \in L^2(c,d).$$

Finally, a final important definition is the compact operators:

Definição 16. *Compact Operator*
The operator $\mathscr{K} : X \to Y$ is called compact if it maps every bounded set S into a relatively compact set $\mathscr{K}(S)$.

A set $M \subset Y$ is called relatively compact if every bounded sequence $(y_j) \subset M$ has an accumulation point in $\overline{M}$, i.e., if the closure $\overline{M}$ is compact. The set of all compact operators from X to Y is a closed subspace of $\mathscr{L}(X,Y)$. In respect to integral operators:

Teorema 17. *Compactness of integral operators*

1. *Let $k \in L^((c,d) \times (a,b))$. The operator $\mathscr{K} : L^2(a,b) \to L^2(c,d)$, defined by*

$$\mathscr{K}\{x(t)\} := \int_a^b k(t,s)x(s)ds, \quad t \in (c,d),\ x \in L^2(a,b) \tag{I.6}$$

   is compact from $L^2(a,b)$ into $L^2(c,d)$.

2. *Let k be continuous on $[c,d] \times [a,b]$ or weakly singular on $[a,b] \times [a,b]$ (in this case $[c,d] = [a,b]$). Then $\mathscr{K}$ defined by* (I.6) *is also compact as an operator from $C[a,b]$ into $C[c,d]$.*

Apêndice J

Shape metrics

In an Electromagnetic Inverse Scattering (EISP) problem, we are interested in detecting objects in an image. These objects have three characteristics: position, shape and contrast value. In the literature of this problem, there are measures to evaluate the error of a method when estimating the contrast of an object. However, up to the date of this thesis, there is no reference for measuring position and shape. This appendix aims to investigate and develop ways to measure the quality of an algorithm in recovering shapes. In addition, this annex is dedicated to analyzing the case of reconstructing a single object within the image.

The identification of objects in an image is a classic problem in the area of Image Processing. Traditionally, the goal is to recognize patterns in figures and to identify those patterns. In EISP, identifying the object is not the purpose, in the sense of comparing it with a database, but only to retrieve shapes. This kind of problem can be addressed with methods known as Marching Squares, which generate contours from a threshold process.

Suppose an algorithm designed to recover an image. The original and the recovered images are show in Figure J.1. If we apply the Marching Squares algorithm do obtain the contours using the same threshold for the recovered image as in Algorithm **??**, we will obtain the results which are in J.2.

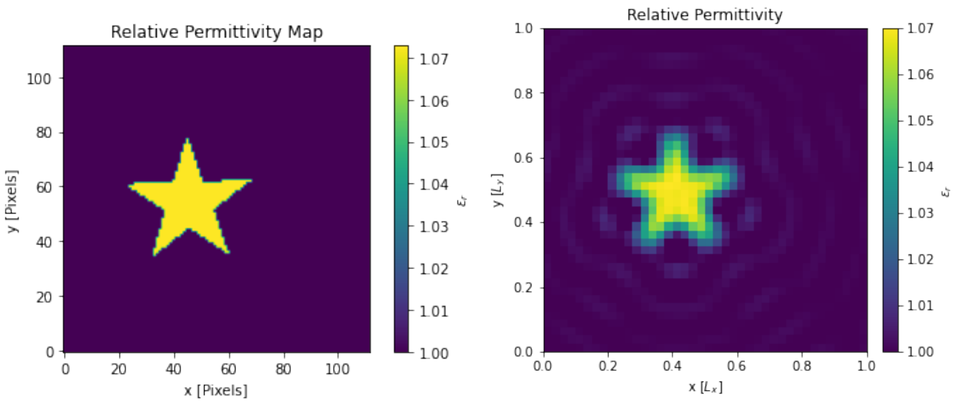

(a) Original (b) Recovered

Figura J.1: Example images for shape metrics.

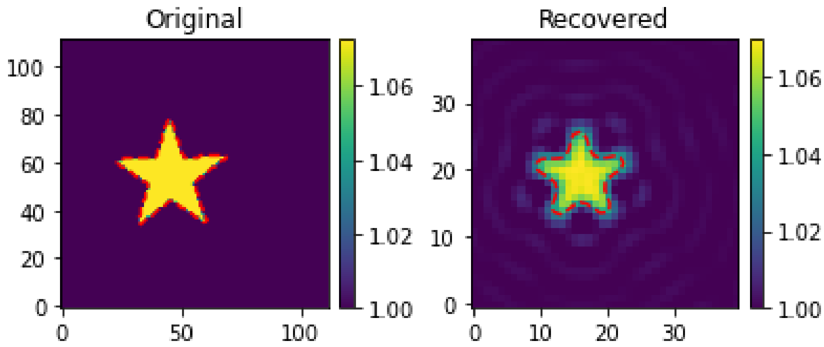

Figura J.2: Contours of original and recovered images.

The main ideia is to calculate the difference area of the two contours. Of course, the area of one minus the area of the other would not work because the two forms might have equal areas but completely different forms. The following algorithm calculates the area of the difference:

1. Calculate the contours;
2. Correct the scale of the recovered contour to be equivalent to the size of the original image;
3. Center the image to isolate the object's position effect;
4. Check which pixels of the image are on each of the objects;
5. Separate those pixels that are in one of the objects and not in the other;
6. Calculate the quantity and multiply by an area element considering the limits equal to 0 and 1.

This algorithm is implemented in the following Python3 code:

```
# Evaluate contourns
co = measure.find_contours(original, 1.0, fully_connected='high')
cr = measure.find_contours(recovered, threshold)

# Converting scale of recovered contourn
for i in range(len(cr)):
cr[i][:, 1] = original.shape[1]*cr[i][:, 1]/recovered.shape[1]
cr[i][:, 0] = original.shape[0]*cr[i][:, 0]/recovered.shape[0]

# Thresholding
masko = np.zeros(original.shape, dtype=bool)
maskr = np.zeros(recovered.shape, dtype=bool)
masko[original > 1] = True
maskr[recovered >= threshold] = True

# Evaluate centers
xo, yo = np.meshgrid(np.arange(0, original.shape[1]),
                     np.arange(0, original.shape[0]))
xr, yr = np.meshgrid(np.linspace(0, original.shape[1]-1, recovered.shape[1]),
                     np.linspace(0, original.shape[0]-1, recovered.shape[0]))
xco = np.sum(masko*xo)/np.sum(masko)
```

```
yco = np.sum(masko*yo)/np.sum(masko)
xcr = np.sum(maskr*xr)/np.sum(maskr)
ycr = np.sum(maskr*yr)/np.sum(maskr)

# Centralization
for i in range(len(co)):
co[i][:, 0] = co[i][:, 0]-yco+original.shape[0]/2
co[i][:, 1] = co[i][:, 1]-xco+original.shape[1]/2

# Centralization
for i in range(len(cr)):
cr[i][:, 0] = cr[i][:, 0]-ycr+original.shape[0]/2
cr[i][:, 1] = cr[i][:, 1]-xcr+original.shape[1]/2

# Verify points
masko = np.zeros(original.shape, dtype=bool)
counter = np.zeros(original.shape)
for i in range(len(co)):
maskt = measure.grid_points_in_poly(original.shape, co[i])
counter[maskt] += 1
masko[np.mod(counter, 2) == 1] = True

# Verify points
maskr = np.zeros(original.shape, dtype=bool)
counter = np.zeros(original.shape)
for i in range(len(cr)):
maskt = measure.grid_points_in_poly(original.shape, cr[i])
counter[maskt] += 1
maskr[np.mod(counter, 2) == 1] = True

# Xor operation
diff = np.logical_xor(masko, maskr)

# Area of the difference
zeta_s = np.sum(diff)/np.sum(masko)*100

# Figure
fig, axis = plt.subplots(ncols=3, figsize=[3*6.4,4.8])
fig.subplots_adjust(wspace=.5)
axis[0].imshow(masko, origin='lower')
axis[0].set_title('Original')
axis[1].imshow(maskr, origin='lower')
axis[1].set_title('Recovered')
axis[2].imshow(diff, origin='lower')
axis[2].set_title('Difference')

plt.show()
```

This code yields results in Figura J.3. The ζ_S measure in this case was 20.68%.

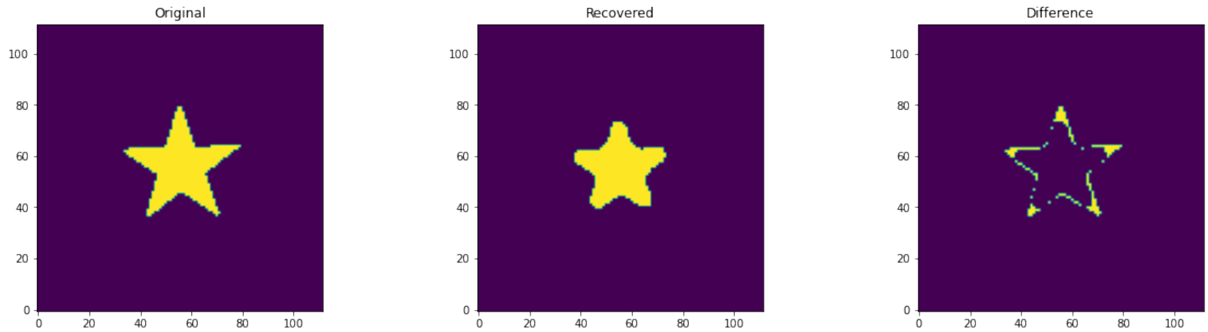

Figura J.3: Original, recovered and difference area.